RESEARCHERID
THOMSON REUTERS

[Rajput* 7(4): April, 2020] ISSN 2349-4506
Impact Factor: 3.799

Global Journal of Engineering Science and Research Management

ANALYTIC STUDY OF STEADY MHD FLOW OF DOUBLE-LAYER OPTICAL FIBER IN A POROUS MEDIUM WITH HEAT TRANSFER

Taimoor Rajput*, Feroz Shah, Fozia Shaikh
* Research Scholar, Mehran University of Engineering and technology Jamshoro, 76090, Pakistan
Professor, Mehran University of Engineering and technology Jamshoro, 76090, Pakistan
Assistant Professor, Mehran University of Engineering and technology Jamshoro, 76090, Pakistan.

DOI: 10.5281/zenodo.3753020

KEYWORDS: Double-layer, Optical fiber, Magneto-hydro-dynamics, wet-on-wet process, porosity, PTT Fluid, Coaxial extrusion, Darcy's permeability, Lorentz force, Axial Direction.

ABSTRACT
Now a days, the coating of double-layer optical fiber attracts many engineers and scientists because of its modern applications which provides the protection for mechanical damage and signal attenuation. In this article, the coating of double-layer optical fiber with magneto-hydro-dynamics (MHD) is performed by using the Phan-Thein-Tanner (PTT) fluid model which is satisfied by melt polymer in a pressure type die using wet-on-wet coating process in a porous medium. Here we assume that PTT fluid model is fully developed. The double-layer immiscible fluid flows is modeled in an annular die, where the fiber is dragged with a sufficient speed. The governing equations for velocity and temperature profiles are solved exactly and the effects of embedded parameters are analyzed graphically.

INTRODUCTION
Fluid, (liquid or gas) which cannot up-holds a tangential or shearing force. that suffers a continuous change in shape when experienced to such a stress. Fluids are basically classified into four classes Ideal, Real, Newtonian and non-Newtonian. Fluids having no viscosity and incompressible are called ideal fluids, but there is no ideal fluid whereas the fluids having some viscosity which are compressible are called real fluid, all fluids are real. The fluids in which viscosity does not change however the temperature varies are known as Newtonian fluids These fluids vary directly with viscosity and shear stress such as water, mineral oil, Alcohol etc. and a fluid whose viscosity changes when shearing force is applied is called non-Newtonian fluid such as ketchup, toothpaste, glue, paint etc.

Flow of fluid has all sorts of aspects. It is very smooth, regular and flows, but usually it is not well disciplined. It is unsettled and starts flowing in random way. In fluid mechanics, fluid's flow is characterized as steady or unsteady, compressible or incompressible, laminar or turbulent, viscous or non-viscous. Some of these characteristics show the properties of flowing liquid itself, and others focus on the movement of fluid. In **steady flow**, the velocity of the fluid doesn't depend upon time. When flow is **unsteady**, the velocity of the fluid can fluctuate between any two nodes and depends upon time. Fluid flow can also be compressible or incompressible, depending on whether its density can be changed or not. Liquids are nearly incompressible whereas gases are compressible. Fluid flow, in which the fluid moves fluently or in regular paths, is called laminar flow whereas flow in which the fluid undergoes irregular variations or mixing is called turbulent flow. Flow of fluid can be viscous or non-viscous. Measure of thickness of the fluid is called Viscosity. It usually varies with temperature. Viscosity is a crucial feature to clarify the state of a fluid's flow.

The Computational Fluid dynamics is a branch of fluid mechanics in which we use numerical techniques to solve fluid flows problems. In Computational fluid dynamics we inspect the fluid flow in commensurate with its physical properties such as velocity, temperature, pressure, density and viscosity. Computational fluid dynamics analyses are frequently used in various engineering for example Aerodynamics and hydrodynamics such as lift, drag or field properties. Modern fluid mechanical problems would be more complex to solve without the use of CFD.

The optical fiber coating is a modern procedure to prevent from insulation, mechanical damage, and environmental protection and oppose to cover signal depletion. Usually, we have three different methods for coating of wire. They are such as

- Electro-statistical deposition process
- Dipping process
- Coaxial extrusion process

The suitable and simple procedure for coating of wire is the coaxial extrusion process which is operated at the maximum wire drawing speed, pressure, and temperature. In this process of coating the melt-polymer and continuum velocity create ultra-pressure in a specific region due to which the result are formed in the shape of fast coating and strong bonding. The production of optical fibers is a series of self-working inline process. Furthermore, the optical fiber production accomplishes as the fluid fiber coatings are cured by Ultraviolet (UV) Lamps and coatings plays a significant role to produce mechanical security and to save from the entrance of moisture into flaws of microscopic level on the surface of fiber.

In this research, I will propose a scheme for porous polymer optical fibers to fabricate them. Here the porosity is introduced by the absorption of PTT fluid in two layers. Up to our knowledge, this production has not been developed previously. The ability of the porous cladding to ingest fluid through capillary force encourages promising applications in the biomedical field. Here, we also used process of the wet-on-wet coating with magneto-hydro-dynamics for optical fiber coating. It is shown in geometry Figure 1). [1] Z.Khan, R.A.Shah, S.Islam et.al. , 2016. Investigated the transferring of heat for steady and incompressible PTT fluid in double-layer coating of optical fiber with slip condition. Exact solution for the velocity flow rates and temperature profile has been obtained. [1] Sang.H.park, Yeong.S.Lee, Ho Sang.K, 2010) Predicted the effect on the process of wet-on-wet coating on two layers of optical fiber. The solutions for relevant parameters were discussed theoretically. [2] H.khan T.Haroon, A.M.Siddiqui examined the extrusion of wire coating of a third grade fluid in pressure-type die.The differential mode is solved by Homotopy perturbation method. [3] Siddiqui A.M et.al. investigated the transferring of heat for steady and incompressible PTT concentric flowing fluid between two immiscible fluid layers with no slip. Exact solutions for the velocity flow rates, stresses and temperature profile has been obtained. [4] Kyoung.J.K, Ho sang. K,. studied the coating of double-layer liquid of non-Newtonian fluid in a manufacturing of optical fiber for the simplified geometry of capillary annulus. Computed the resin velocity profiles on different non-Newtonian parameter. [5] M.Elahi, R.A.shah, et.al. stratified the steady flow of third order fluid with post-treatment the coating of wire. Solutions for transferring of heat flows and velocity profile are determined by OHAM and regular perturbation method. [6] S.Asgher, M.Ayub., et.al. investigated the rotating flow of a third order fluid with the effects of partial slip in a porous medium. The differential model was solved by homotopy analysis method (HAM). [7] Umavathi, J.C., et.al. analyzed the temperature profile past in an open inclined with magneto-hydro-dynamic in which one phase was electrically conducting. The results of the thermal conductivities and the ratios of viscosities at different parameters are obtained by perturbation method. [8] Siddiqui A.M et.al. examined the exact solution of n-concentric viscous fluid layers in a pipe. The effects of appropriate parameters on the velocity profiles have been presented graphically for two-layers and multi-layers flows. [9] I.Khan, Zeeshan, T.Gul,.; et.al examined the two-layers coating of optical fiber glass for PTT fluid model. The Exact solutions were obtained for temperature and velocity profiles.

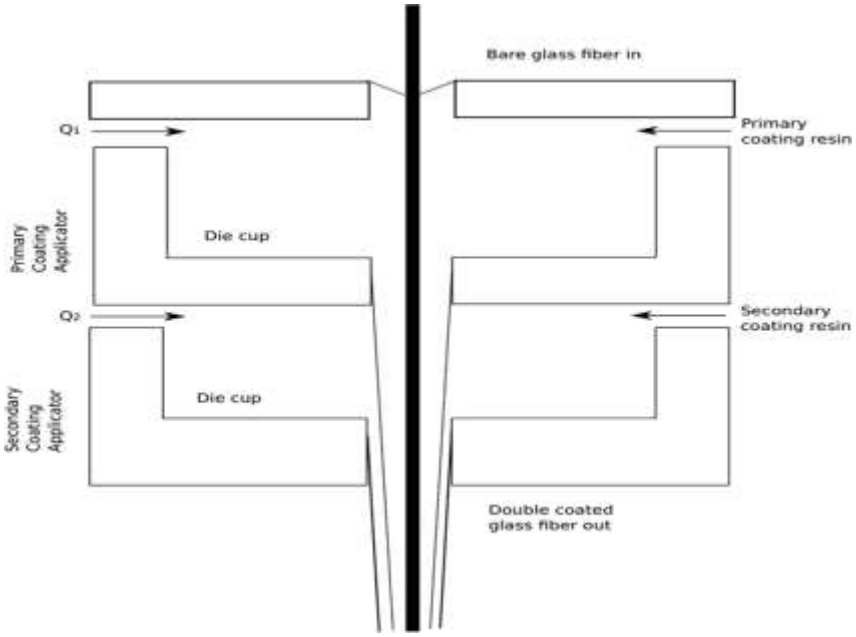

Figure 1

MODELING OF THE PROBLEM

Consider a model of concentric double-layer flow in a die of length L, the pressure is applied on fiber and die which are concentric. Here the system of coordinate is chosen at the center of the optical fiber, where r is taken perpendicular to the flowing direction which is z. We consider the two immicible concentric unidirectional flow of incompressible PTT fluids for a coating of double-layer optical fiber where fiber is covered by pressurized fluid. The optical fiber of radius R is kept at a steady temperature Θ. Furhter the process of coating is carried out into two stages. In the first stage the uncovered optical fiber of radius R_w is dragged with uniform velocity U into the primary coating liquid. In the next stage we pass the wet coating through the secondary coating die of the radius of radius R_d. Due to which the fiber becomes the double-layer coating system. The ultraviolet (UV) lamps are used to dried up the wet layers as shown in the given geometry,

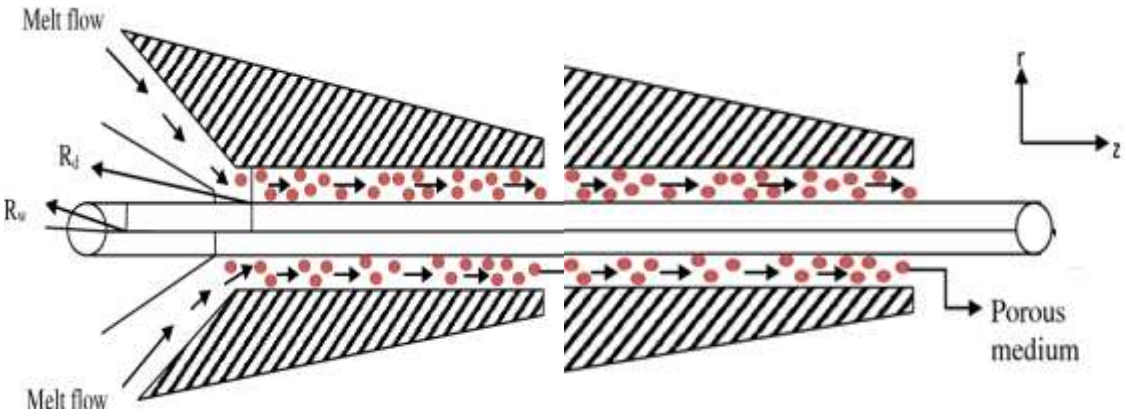

Figure 2

Here we assume the unidirectional, steady, and fully developed flow. The extra stresses and velocities are assumed to be:

$\tau^{(n)} = \tau^{(n)}(r)$ and $V^{(n)} = [0, 0, v^{(n)}(r)]$, $n = 1, 2$ (1)

Boundary conditions are:

$$\left.\begin{array}{l} w = U_w \ , \quad \Theta = \Theta_w \quad at \quad r = R_w \\ w = U_d \ , \quad \Theta = \Theta_d \quad at \quad r = R_d \end{array}\right\} \quad (2)$$

The general form of the constitutive equation which defines the PTT fluid is:

$$f\left(tr(\tau^{(n)})\right)\tau^{(n)} + \lambda^{(n)}\hat{\tau}^{(n)} = 2\mu^{(n)}{A_1}^{(n)}, \qquad n = 1,2 \quad (3)$$

Where $\mu^{(n)}$ and $\lambda^{(n)}$ the coefficients of viscosity and relaxation time of the nth fluid, $tr(\tau^{(n)})$ Is the trace of stress tensor $\tau^{(n)}$ and ${A_1}^{(n)}$ is the deformation rate tensor defined by:

$${A_1}^{(n)} = \frac{1}{2}\left[L^{(n)} + \left(L^{(n)}\right)^T\right]; \qquad n = 1,2 \quad (4)$$

The upper convected derivative term $\hat{\tau}^{(n)}$ can be expressed as:

$$\hat{\tau}^{(n)} = \frac{d\hat{\tau}^{(n)}}{dt} - \tau^{(n)}.L^{(n)} - \left(L^{(n)}\right)^T.\tau^{(n)}\ ; \qquad n = 1,2 \quad (5)$$

A mathematical linear form of PTT model of function f by the tanner's classification is:

$$f\left(tr(\tau^{(n)})\right) = 1 + \frac{\varepsilon^{(n)}\lambda^{(n)}}{\mu^{(n)}}tr(\tau^{(n)})\ ; \qquad n = 1,2 \quad (6)$$

Where is $\varepsilon^{(n)}$ a parameter related to extended form of the fluid model.

The fundamental equations which govern the non-isothermal flow of two immiscible, incompressible fluids are the continuity equation, the law of conservation of momentum, and the law of conservation of energy. Mathematically,

$$divV^{(n)} = 0, \qquad n = 1,2 \quad (7)$$

$$\rho^{(n)}\frac{dV^{(n)}}{dt} = div\tau^{(n)} - grad\ p + J \times B - \mu^{(n)}\frac{\emptyset V^{(n)}}{K_p} \qquad n = 1,2 \quad (8)$$

$$\rho^{(n)}C_p^{(n)}\frac{d\Theta^{(n)}}{dt} = K^{(n)}\nabla^2\Theta^{(n)} + T^{(n)}.L^{(n)} \qquad n = 1,2 \quad (9)$$

Here n denotes the number of fluids, ρ is the constant fluid density, V is the velocity vector, τ is the extra stress tensor, C_p is the specific heat of the fluid, Θ denotes the temperature of fluid, K represents the thermal conductivity, p is dynamic pressure, $T^{(n)} = -p\mathrm{I} + \tau^{(n)}$ is the Cauchy stress tensor of nth fluid, μ is co-efficient of viscosity, ϕ and K_p show the porosity and darcy's permeability respectively, $\frac{d}{dt}$ denotes the material time derivative, L is gradient of V and the term of body force corresponds to magneto-hydro-dynamic flow is the lorentz force $\boldsymbol{J} \times \boldsymbol{B}$, where B is induced magnetic field and J shows the density of current, using Ohm's law and According to our statement magnetic field reduces to;

$$J \times B = \left(0,0,-\sigma B^2 v(r)\right) \quad (10)$$

From the eq. (1), the continuity eq. (7) identically satisfied and from eq. (10) we arrive at,

$$\frac{\partial p}{\partial r} = 0, \quad (11)$$

$$\frac{\partial p}{\partial \Theta} = 0, \quad (12)$$

$$\frac{\partial p}{\partial z} = \frac{1}{r}\frac{d}{dr}\left(r\,\tau_{rz}^{(n)}\right), \quad (13)$$

$$k^{(n)}\left(\frac{d^2}{dr^2} + \frac{1}{r}\frac{d}{dr}\right)\Theta^{(n)} + \tau_{rz}^{(n)}\frac{dw^{(n)}}{dr} = 0 \quad (14)$$

$$f\left(tr(\tau^{(n)})\right)\tau_{zz}^{(n)} = 2\lambda\,\tau_{rz}^{(n)}\frac{dw^{(n)}}{dr} \quad (15)$$

$$f\left(tr(\tau^{(n)})\right)\tau_{rz}^{(n)} = \mu^{(n)}\frac{dw^{(n)}}{dr} \quad (16)$$

$$\Phi = \tau_{rz}^{(n)}\frac{dw^{(n)}}{dr} \quad (17)$$

From eq. (11) and (12) it is concluded that p is a function of z only, by consideration the pressure gradient along the axial direction in constant. Thus we have $\frac{dp}{dz} = \Gamma$
After integrating eq. (13) with respect to r we get,

$$\tau_{rz}^{(n)} = \frac{\mathrm{r}}{2}\left[\Gamma + \delta B^2 w + \frac{\mu w}{K_p}\right] + \frac{C^{(n)}}{r}, \quad (18)$$

Here $C^{(n)}$ is an arbitrary constant of integration, by inserting eq. (18) in eq. (16), we have

$$f\left(tr(\tau^{(n)})\right) = \frac{\mu^{(n)}\frac{dw^{(n)}}{dr}}{\frac{\mathrm{r}}{2}\left[\Gamma + \delta B^2 w + \frac{\mu w}{K_p}\right] + \frac{C^{(n)}}{r}} \quad (19)$$

Combining eq. (15), (16) & (18) we arrive at the explicit expressions for a normal stress component τ_{zz} as

$$\tau_{zz}^{(n)} = 2\frac{\lambda}{\mu^{(n)}}\left(\frac{\Gamma}{2}r + \frac{C^{(n)}}{r} + r\delta Bw + \frac{r\mu w}{K_p}\right)^2 \quad (20)$$

From eq. (9) and (19), we have

$$\mu^{(n)}\frac{dw^{(n)}}{dr} = \left[1 + \frac{\varepsilon^{(n)}\lambda^{(n)}}{\mu^{(n)}}\left\{2\frac{\lambda}{\mu}\left(\frac{\Gamma}{2}r + \frac{C^{(n)}}{r} + r\delta Bw + \frac{r\mu w}{K_p}\right)^2\right\}\right]\left[\frac{\Gamma}{2}r + \frac{C^{(n)}}{r} + r\delta Bw + \frac{r\mu w}{K_p}\right] \quad (21)$$

Substituting eq. (20) in (21) we get an analytical equation for axial velocity as

$$\frac{dw^{(n)}}{dr} = \frac{1}{\mu^{(n)}}\left(\frac{\Gamma}{2}r + \frac{C^{(n)}}{r} + B(rw) + (rw)\frac{\mu}{K_p}\right) + 2\epsilon\frac{\lambda^2}{\mu^{3\,(n)}}\left(\frac{\Gamma}{2}r + \frac{C^{(n)}}{r} + r\delta Bw + \frac{r\mu w}{K_p}\right)^3 \quad (22)$$

And the temperature distribution is:

$$k^{(n)}\left(\frac{d^2}{dr^2} + \frac{1}{r}\frac{d}{dr}\right)\Theta^{(n)} + \tau_{rz}^{(n)}\frac{dw^{(n)}}{dr} = 0, \quad (23)$$

The boundary conditions on $\Theta^{(n)}$ is $\widehat{\Theta}_w$ at the fiber optics and $\widehat{\Theta}_d$ at the wall and boundary and interface conditions on the temperature are

$$\Theta_1 = \widehat{\Theta}_w \quad at \quad r = R_w \quad and \quad \Theta_2 = \widehat{\Theta}_d \quad at \quad r = R_d \quad (24)$$

$$\Theta_1 = \Theta_2 \ and \ k_1\frac{d\Theta_1}{dr} = k_2\frac{d\Theta_2}{dr} \quad at \quad r = R \quad (25)$$

By introducing the non-dimensional flow variables as

$$r^* = \frac{r}{R_w}, \quad w^{*(n)} = \frac{w^{(n)}}{U}, \quad \Theta^{*(n)} = \frac{\Theta^{(n)} - \widehat{\Theta}_d}{\widehat{\Theta}_d - \widehat{\Theta}_w}, \quad C^{*(n)} = \frac{2C^{(n)}}{R_w^2\Gamma}, \quad \Omega^* = \frac{R}{R_w}$$

$$Br^{(n)} = \frac{\mu^{(n)}U^2}{k^{(n)}\left(\widehat{\Theta}_d - \widehat{\Theta}_w\right)}, \quad D^{2\,(n)} = \frac{\lambda V_c}{R_w}, \quad X^{(n)} = \frac{V_c}{U}, \quad K = \frac{k_2}{k_1}, \ n = 1,2$$

$$\gamma^{*(n)} = \frac{\gamma R_w}{\mu^{(n)}}, \quad \frac{R_d}{R_w} = \delta > 1, \quad M^2 = \frac{\delta B^2 R_w^2}{\mu}, \quad K_p = \frac{R_w^2}{U_w K_p^*} \quad (26)$$

$$\frac{dw^{(n)}}{dr}=\left[-384X^{(n)}\varepsilon D^{2\,(n)}C^{(n)}-128X^{(n)}\varepsilon D^{2\,(n)}C^{(n)}M\omega+\frac{192\varepsilon D^{2\,(n)}C^{(n)}\omega}{K}-384X^{(n)}\varepsilon M\omega^2D^{2\,(n)}C^{(n)}-\frac{24\varepsilon D^{2\,(n)}C^{(n)}\omega}{KX^{(n)}}-4X^{(n)}-4M\omega X+\frac{\omega}{K}\right]r-4C^{(n)}X^{(n)}\frac{1}{r}+\left\{-128X^{(n)}\varepsilon D^{2\,(n)}-512X^{(n)}\varepsilon D^{2\,(n)}M^2\omega^2+\frac{2\varepsilon D^{2\,(n)}\omega^3}{K^3X^{2\,(n)}}+\frac{96\varepsilon D^{2\,(n)}M^2\omega^2}{K}+\frac{24\varepsilon D^{2\,(n)}M\omega^3}{K^2}-384X^{(n)}\varepsilon D^{2\,(n)}M\omega-\frac{192X^{(n)}\varepsilon D^{2\,(n)}\omega}{K}-\frac{24X^{(n)}\varepsilon D^{2\,(n)}M^2\omega^2}{K^2X^{(n)}}+\frac{192\varepsilon D^{2\,(n)}M\omega^2}{K}\right\}r^3+\left\{-384X^{(n)}C^{2\,(n)}\varepsilon D^{2\,(n)}-384X^{(n)}\varepsilon M\omega D^{2\,(n)}C^{2\,(n)}+\frac{96\varepsilon\omega D^{2\,(n)}C^{(n)}}{K}-4X^{(n)}C^{(n)}\right\}\frac{1}{r}-\{128C^{3\,(n)}X^{(n)}\varepsilon D^{2\,(n)}\}\frac{1}{r^3} \quad (27)$$

$$\frac{d}{dr}\left(r\frac{d\Theta^{(n)}}{dr}\right)-4Br^{(n)}X^{(n)}\left(r^2+C^{(n)}\right)\frac{dw^{(n)}}{dr}=0 \quad (28)$$

$$w_1(1)=1-4\gamma_1X_1(C_1),\quad w_2(\delta)=4\gamma_2X_2\left(\delta+\frac{C_2}{\delta}\right) \quad (29)$$

$$w_1(\Omega)=w_2(\Omega),\quad \tau_{rz_1}(\Omega)=\tau_{rz_2}(\Omega) \quad (30)$$

$$\Theta_1(1)=0,\ \Theta_2(\delta)=1,\quad \Theta_1(\Omega)=\Theta_2(\Omega),\quad \frac{d\Theta_1(\Omega)}{dr}=K\frac{d\Theta_2(\Omega)}{dr} \quad (31)$$

Here $V_c=-R_w^2\frac{\Gamma}{8\mu^{(n)}}$ is the characteristics velocity scale, $\varepsilon D^{2\,(n)}$ is the characteristic Deborah number based on velocity scale Vc, $X^{(n)}$ has physical meaning of a non-dimensional pressure gradient and $Br^{(n)}$ is the Brinkman number and $n=1,2$ stands for primary and secondary coating layer flows respectively.

SOLUTION OF THE PROBLEM

To obtain the solution for the velocity field and temperature distribution for both layers, we solve Equations (27) and (28), corresponding to the boundary conditions given by equations (29-31) respectively.
Primary layer velocity field, flow rate, thickness of the coated fiber optics and temperature are:

$$w^1=\left[-192X^{(n)}\varepsilon D^{2\,(n)}C^{(n)}-64X^{(n)}\varepsilon D^{2\,(n)}C^{(n)}M\omega+\frac{96\varepsilon D^{2\,(n)}C^{(n)}\omega}{K}-192X^{(n)}\varepsilon M\omega^2D^{2\,(n)}C^{(n)}-\frac{12\varepsilon D^{2\,(n)}C^{(n)}\omega}{KX^{(n)}}-2X^{(n)}-2M\omega X+\frac{\omega}{2K}\right]r^2+2C^{(n)}X^{(n)}\frac{1}{r^2}+\left\{-32X^{(n)}\varepsilon D^{2\,(n)}-128X^{(n)}\varepsilon D^{2\,(n)}M^2\omega^2+\frac{\varepsilon D^{2\,(n)}\omega^3}{2K^3X^{2\,(n)}}+\frac{24\varepsilon D^{2\,(n)}M^2\omega^2}{K}+\frac{6\varepsilon D^{2\,(n)}M\omega^3}{K^2}-96X^{(n)}\varepsilon D^{2\,(n)}M\omega-\frac{48X^{(n)}\varepsilon D^{2\,(n)}\omega}{K}-\frac{6X^{(n)}\varepsilon D^{2\,(n)}M^2\omega^2}{K^2X^{(n)}}+\frac{48\varepsilon D^{2\,(n)}M\omega^2}{K}\right\}r^4+\left\{192X^{(n)}C^{2\,(n)}\varepsilon D^{2\,(n)}+192X^{(n)}\varepsilon M\omega D^{2\,(n)}C^{2\,(n)}-\frac{48\varepsilon\omega D^{2\,(n)}C^{(n)}}{K}+2X^{(n)}C^{(n)}\right\}\frac{1}{r^2}+\{30C^{3\,(n)}X^{(n)}\varepsilon D^{2\,(n)}\}\frac{1}{r^4}+C_3 \quad (32)$$

$$Q^{(1)}=\left\{X^{(1)}\left(C^{(1)}+96C^{2\,(1)}\varepsilon D^{2\,(1)}+\frac{1}{r}C^{(3)}\right)(\Omega^2-1)-\left(\frac{1}{2}+48C^{(1)}\varepsilon D^{2\,(1)}\right)(\Omega^4-1)-\frac{16}{3}\varepsilon D^{2\,(1)}(\Omega^6-1)+64C^{3\,(1)}\varepsilon D^{2\,(1)}ln\Omega-2\left(K^{\alpha}+96C^{2\,(1)}\varepsilon D^{2\,(1)}\right)\Omega^2ln\Omega\right\} \quad (33)$$

$$R^{(1)} = \left[\left\{1 - \frac{2}{15\Omega}2\left(96\varepsilon D^{2\,(1)}\left(-\Omega + \Omega^6 + 10(-1+\Omega)C^{(1)}\left(\Omega + \Omega^2 + \Omega^3 + 6lnr\Omega C^{(1)} - C^{2\,(1)}\right)X^{(1)}\right)\right.\right.$$
$$\left.\left. + 5\Omega\left(-3(-1+\Omega)C^{(3)} + 6\ln(-1+\Omega^2)\,C^{(1)}X^{(1)} + 2(-1+\Omega^3)X^{(1)}\right)\right)\right\}\Bigg]^{\frac{1}{2}} \quad (34)$$

$$\Theta^{(1)} = -4Br^{(1)}X^{2\,(1)}\left(-\frac{1}{4}r^4 - 3K^{(\alpha)}r^2 - \frac{32}{9}\varepsilon D^{2\,(1)}r^6 - 32K^{(\alpha)}\varepsilon D^{2\,(1)}r^4 - 96K^{2\,(\alpha)}\varepsilon D^{2\,(1)}r^2\right.$$
$$- 128K^{3\,(\alpha)}X^{(1)}\varepsilon D^{2\,(1)}lnr - 4K^{2\,(\alpha)}lnr - 8\varepsilon D^{2\,(1)}r^4 - 96K^{2\,(\alpha)}\varepsilon D^{2\,(1)}r^2$$
$$\left. - 384K^{3\,(\alpha)}\varepsilon D^{2\,(1)}lnr + 32K^{3\,(\alpha)}\varepsilon D^{2\,(1)}\frac{1}{r^2}\right) + D^{(1)}lnr + D_2 \quad (35)$$

Secondary layer velocity field, flow rate, thickness of the coated fiber optics and temperature are.

$$w^2 = \left[-192X^{(n)}\varepsilon D^{2\,(n)}C^{(n)} - 64X^{(n)}\varepsilon D^{2\,(n)}C^{(n)}M\omega + \frac{96\varepsilon D^{2\,(n)}C^{(n)}\omega}{K} - 192X^{(n)}\varepsilon M\omega^2 D^{2\,(n)}C^{(n)}\right.$$
$$\left. - \frac{12\varepsilon D^{2\,(n)}C^{(n)}\omega}{KX^{(n)}} - 2X^{(n)} - 2M\omega X + \frac{\omega}{2K}\right]r^2 + 2C^{(n)}X^{(n)}\frac{1}{r^2}$$
$$+ \left\{-32X^{(n)}\varepsilon D^{2\,(n)} - 128X^{(n)}\varepsilon D^{2\,(n)}M^2\omega^2 + \frac{\varepsilon D^{2\,(n)}\omega^3}{2K^3X^{2\,(n)}} + \frac{24\varepsilon D^{2\,(n)}M^2\omega^2}{K} + \frac{6\varepsilon D^{2\,(n)}M\omega^3}{K^2}\right.$$
$$\left. - 96X^{(n)}\varepsilon D^{2\,(n)}M\omega - \frac{48X^{(n)}\varepsilon D^{2\,(n)}\omega}{K} - \frac{6X^{(n)}\varepsilon D^{2\,(n)}M^2\omega^2}{K^2X^{(n)}} + \frac{48\varepsilon D^{2\,(n)}M\omega^2}{K}\right\}r^4$$
$$+ \left\{192X^{(n)}C^{2\,(n)}\varepsilon D^{2\,(n)} + 192X^{(n)}\varepsilon M\omega D^{2\,(n)}C^{2\,(n)} - \frac{48\varepsilon\omega D^{2\,(n)}C^{(n)}}{K} + 2X^{(n)}C^{(n)}\right\}\frac{1}{r^2}$$
$$+ \left\{30C^{3\,(n)}X^{(n)}\varepsilon D^{2\,(n)}\right\}\frac{1}{r^4} + C_4 \quad (36)$$

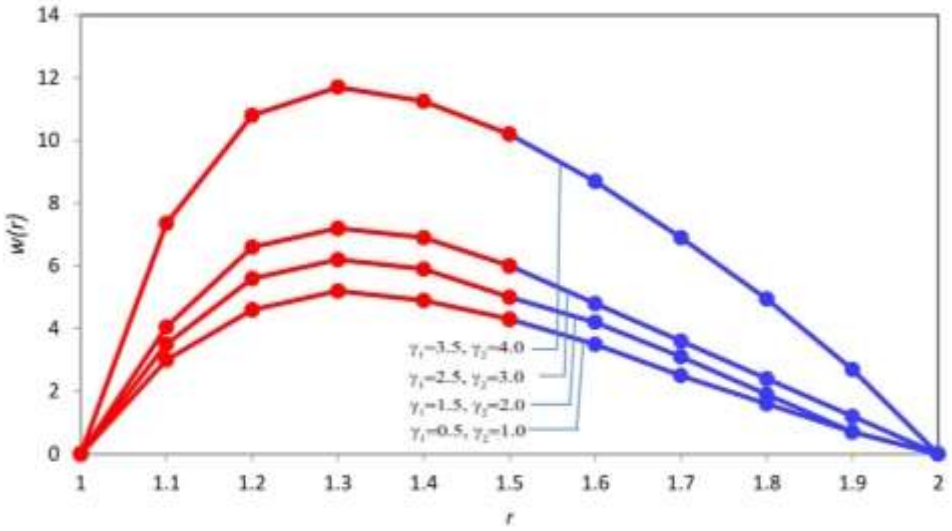

Figure 3

Figure 3: Varia $=$
$\mathbf{1.5}, \boldsymbol{\varepsilon D^{2\,(1)}} = \mathbf{5}, \quad \boldsymbol{\varepsilon D^{2\,(1)}} = \mathbf{10}\,, \boldsymbol{\delta} = \mathbf{2}, \quad \boldsymbol{M} = \mathbf{0.2}, \quad \boldsymbol{\omega} = \mathbf{0.1}, \quad \boldsymbol{K_p} = \mathbf{2}, \quad \boldsymbol{\Omega} = \mathbf{0.1}, \quad \boldsymbol{\mu} = \mathbf{1,2}$

$$Q^{(2)} = C^{(4)}(\delta^2 - \Omega^2) - \frac{1}{2}X^{(2)}\left(1 + 96C^{(2)}\varepsilon D^{2\,(2)}\right)(\delta^4 - \Omega^4) - \frac{16}{3}X^{(2)}\varepsilon D^{2\,(2)}(\delta^6 - \Omega^6)$$
$$- 2C^{(2)}X^{(2)}\left(1 + 192\varepsilon D^{2\,(2)}\right)(\delta^2 ln\delta - \Omega^2 ln\Omega) + 64C^{2\,(2)}\varepsilon D^{2\,(2)}(ln\delta - ln\Omega) \quad (37)$$

$$R^{(2)} = \Big[1 - \frac{1}{15\Omega}2\big[15\delta\Omega(-\delta+\Omega)C^{(4)} + 6\big(5ln\delta(\delta-\Omega)\Omega(\delta+\Omega)C^{(3)} + 16\varepsilon D^{2\,(2)}\big(\delta^6\Omega - \delta\Omega^6 + 10(\delta-\Omega)\big)C^{(3)}\delta\Omega(\delta^2+\delta\Omega+\Omega^2) + 6lnr\delta\Omega K^{(c)} - C^{2\,(3)}\big) + 10\delta\Omega(\delta^3-\Omega^3)X^{(2)}\big]\Big]^{\frac{1}{2}} \quad (38)$$

$$\Theta^{(2)} = -4Br^{(2)}X^{2\,(2)}\Big(-\frac{1}{4}r^4 - 3C^{(3)}r^2 - \frac{32}{9}\varepsilon D^{2\,(2)}r^6 - 24C^{(3)}\varepsilon D^{2\,(2)}r^4 - 96C^{2\,(3)}\varepsilon D^{2\,(2)}r^2 - 128C^{3\,(3)}X^{(2)}\varepsilon D^{2\,(2)}lnr - 4C^{2\,(3)}lnr - 8\varepsilon D^{2\,(2)}r^4 - 96C^{2\,(3)}\varepsilon D^{2\,(2)}r^2 - 384C^{3\,(3)}\varepsilon D^{2\,(2)}lnr + 32C^{3\,(3)}\varepsilon D^{2\,(2)}\frac{1}{r^2}\Big) + D^{(3)}lnr + D_4 \quad (39)$$

Where $C^{(1)}$, $C^{(2)}$, $C^{(3)}$,C_4, $D^{(1)}$, $D^{(2)}$, $D^{(3)}$and D_4 are all constants given below.

$$C^{(1)} = -\frac{H_1}{3} - \frac{2^{\frac{1}{3}}(-H_1^2+3H_2)}{3\Big[-2H_1^3+9H_1H_2-27H_3+3\sqrt{3}\times\sqrt{-H_1^2H_2^2+4H_1^3H_3-H_1H_2H_3+27H_3^2}\Big]^{\frac{1}{3}}} + \frac{\Big[-2H_1^3+9H_1H_2-27H_3+3\sqrt{3}\times\sqrt{-H_1^2H_2^2+4H_1^3H_3-H_1H_2H_3+27H_3^2}\Big]^{\frac{1}{3}}}{32^{\frac{1}{3}}}, \quad (40)$$

$$C^{(3)} = 1 + 2X^{(1)} + 32\varepsilon D^{2\,(1)} + 192C^{(1)}\varepsilon D^{2\,(1)} - 64C^{(1)}\varepsilon D^{2\,(1)} + 4\gamma_1X^{(1)}\big(1+C^{(1)}\big), \quad (41)$$

$$C^{(2)} = C^{(3)} \quad (42)$$

$$C_4 = 2\delta^2X^{(2)} + 4C^{(3)}X^{(2)}\ln\delta + 32X^{(2)}\varepsilon D^{2\,(2)}\delta^4 + 192X^{(2)}\varepsilon D^{2\,(2)}C^{(2)}\delta^2 + 384X^{(2)}C^{2\,(2)}\varepsilon D^{2\,(2)}ln\delta - 64C^{3\,(2)}X^{(2)}\varepsilon D^{2\,(2)}\frac{1}{\delta^2} + 4\gamma_2X^{(2)}\left(\delta + \frac{C^{(3)}}{\delta}\right), \quad (43)$$

$$D^{(1)} = 4Br^{(1)}X^{2\,(1)}K[(ln\Omega - ln\delta) + \Omega] \times \Big[\frac{1}{4}\delta^4 + 3C^{(1)}\delta^2 + \frac{32}{9}\varepsilon D^{2\,(1)}\delta^6 + 24C^{(1)}D^{2\,(1)}\delta^4 + 96K^{2\,(\alpha)}\varepsilon D^{2\,(1)}\delta^2 + 128C^{3\,(1)}\varepsilon D^{2\,(1)}ln\Omega + 4C^{2\,(1)}ln\Omega + 8\varepsilon D^{2\,(1)}\delta^4 + 96C^{2\,(1)}\varepsilon D^{2\,(1)}\Omega^2 + 384C^{3\,(1)}\varepsilon D^{(1)}ln\Omega - 32C^{3\,(1)}D^{2\,(1)}\frac{1}{\Omega^2}\Big] + 4Br^{(2)}X^{2\,(2)}\Big[\Big[\Omega - \Big(\frac{1}{\Omega} + \frac{1}{\Omega^2ln\Omega}\Big)\Big]\Big] \times \Big[\frac{1}{4}\Omega^4 + 3C^{(3)}\Omega^2 + \frac{32}{9}\varepsilon D^{2\,(2)}\Omega^6 + 24C^{(3)}\varepsilon D^{2\,(2)}\Omega^4 - 96C^{2\,(3)}\varepsilon D^{(1)}\Omega^2 + 128C^{2\,(3)}\varepsilon D^{2\,(2)}ln\Omega + 4C^{2\,(3)}ln\Omega + 8\varepsilon D^{2\,(2)}\Omega^4 + 96C^{2\,(3)}\varepsilon D^{2\,(2)}\Omega^2 + 384C^{3\,(3)}\varepsilon D^{(2)}ln\Omega - 32C^{3\,(3)}\varepsilon D^{2\,(2)}\frac{1}{\Omega^2}\Big] + 4Br^{(1)}X^{2\,(1)}\frac{1}{\Omega^2ln\Omega}\Big(\frac{1}{4} + 3C^{(1)} + \frac{32}{9}\varepsilon D^{2\,(1)} + 32\varepsilon C^{(1)}D^{2\,(1)} + 192C^{2\,(1)}\varepsilon D^{2\,(1)} - 32C^{3\,(1)}\varepsilon D^{2\,(1)}\Big), \quad (44)$$

$$D^{(2)} = 4Br^{(1)}X^{2\,(1)}\frac{1}{\Omega^2ln\delta}\Big(\frac{1}{4} + 3C^{(1)} + \frac{32}{9}\varepsilon D^{2\,(1)} + 32\varepsilon C^{(1)}D^{2\,(1)} + 192C^{2\,(1)}\varepsilon D^{2\,(1)} - 32C^{3\,(1)}\varepsilon D^{2\,(1)}\Big) \quad (45)$$

$$D^{(3)} = 4Br^{(1)}X^{2\,(1)}\Omega(ln\Omega - ln\delta) \times \left[\Omega^3 + 3C^{(1)}\Omega + \frac{64}{3}\varepsilon D^{2\,(1)}\Omega^5 + 96\varepsilon D^{2\,(1)}\Omega^3 + 192C^{2\,(1)}\varepsilon D^{2\,(1)}\Omega + 128C^{3\,(1)}\varepsilon D^{2\,(1)}\frac{1}{\Omega} + 4C^{2\,(1)}\frac{1}{\Omega} + 32\varepsilon D^{2\,(1)}\Omega^3 + 192C^{2\,(1)}\varepsilon D^{2\,(1)}\Omega + 384C^{3\,(1)}\varepsilon D^{(1)}\frac{1}{\Omega} + 64C^{2\,(1)}\varepsilon D^{2\,(1)}\frac{1}{\Omega^3}\right] + 4Br^{(1)}X^{2\,(1)}\frac{1}{ln\delta}\left(\frac{1}{4} + 3C^{(1)} + \frac{32}{9}\varepsilon D^{2\,(1)} + 32\varepsilon C^{(1)}D^{2\,(1)} + 192C^{2\,(1)}\varepsilon D^{2\,(1)} - 32C^{3\,(1)}\varepsilon D^{2\,(1)}\right) + 4Br^{(2)}X^{2\,(2)}\left(\Omega\mathrm{K}(ln\Omega - ln\delta) + \frac{1}{ln\delta}\right) \times \left[\frac{1}{4}\Omega^4 + 3C^{(3)}\Omega^2 + \frac{32}{9}\varepsilon D^{2\,(2)}\Omega^6 + 24C^{(3)}\varepsilon D^{2\,(2)}\Omega^4 - 96C^{2\,(3)}\varepsilon D^{2\,(2)}\Omega^2 + 128C^{3\,(3)}\varepsilon D^{2\,(2)}ln\Omega + 4C^{2\,(3)}ln\Omega + 8\varepsilon D^{2\,(2)}\Omega^4 + 96C^{2\,(3)}\varepsilon D^{2\,(2)}\Omega^2 + 384C^{3\,(3)}\varepsilon D^{(2)}ln\Omega - 32C^{3\,(3)}\varepsilon D^{2\,(2)}\frac{1}{\Omega^2}\right] \quad (46)$$

$$D_4 = 4Br^{(2)}X^{2\,(2)} \times \left[\frac{1}{4}\Omega^4 + 3C^{(3)}\Omega^2 + \frac{32}{9}\varepsilon D^{2\,(2)}\Omega^6 + 24C^{(3)}\varepsilon D^{2\,(2)}\Omega^4 - 96C^{2\,(3)}\varepsilon D^{2\,(2)}\Omega^2 + 128C^{3\,(3)}\varepsilon D^{2\,(2)}ln\Omega + 4C^{2\,(3)}ln\Omega + 8\varepsilon D^{2\,(2)}\Omega^4 + 96C^{2\,(3)}\varepsilon D^{2\,(2)}\Omega^2 + 384C^{3\,(3)}\varepsilon D^{(2)}ln\Omega - 32C^{3\,(3)}\varepsilon D^{2\,(2)}\frac{1}{\Omega^2}\right] - \Omega D^{(3)} \quad (47)$$

Where

$$H_1 = \frac{A_2 + B_2}{A_3 + B_3}, \quad H_2 = \frac{A_1 + B_1}{A_3 + B_3}, \quad H_3 = \frac{G}{A_3 + B_3}$$

$$A_1 = -4X^{(1)}ln\Omega - 192X^{(2)}\varepsilon D^{2\,(2)} - 192X^{(2)}\varepsilon D^{2\,(1)}\Omega - 4\gamma_1 X^{(1)}$$

$$A_2 = -384X^{(1)}\varepsilon D^{2\,(1)}ln\Omega$$

$$A_3 = 64X^{(1)}\varepsilon D^{2\,(1)}\left(\frac{1}{\Omega^2} - 1\right)$$

$$B_1 = 4X^{(2)}ln\Omega + 192X^{(2)}\varepsilon D^{2\,(2)}\Omega^2$$

$$B_2 = 384X^{(2)}\varepsilon D^{2\,(2)}ln\delta + 192X^{(2)}\varepsilon D^{2\,(2)}\Omega^2 - 4\gamma^{(1)}X^{(2)}\frac{1}{\delta}$$

$$B_3 = -64X^{(2)}\varepsilon D^{2\,(2)}\Omega^2\left(\frac{1}{\delta^2} + \frac{1}{\Omega^2}\right)$$

$$G = 1 + 2X^{(1)} + 32X^{(1)}\acute{o}D^{2\,(1)} - 2X^{(2)}\delta^2 - 2X^{(1)}\Omega^2 - 32X^{(2)}\acute{o}D^{2\,(2)}\delta^4 - 32X^{(1)}\acute{o}D^{2\,(1)}\Omega^4 - 2X^{(1)}\Omega^3 + 4\gamma^{(1)}X^{(1)} + 4\gamma^{(2)}X^{(2)}\delta$$

RESULTS AND DISCUSSIONS

The exact results are obtained by solving Equations (27) and (28) along with boundary conditions given by equations (29)– (31) for the velocity and temperature profiles, for the two layers (primary and secondary), related to double-layer optical fiber coating process using melt polymer satisfying Phan-Thien-Tanner (PTT) fluid model in a pressure type die. Wet-on-wet coating process is applied for double-layer optical fiber coating. The effects of different non-dimensional parameters such as, slip parameters, Deborah numbers $\varepsilon D^{2\,(1)}$ and $\varepsilon D^{2\,(2)}$ velocity ratio (ratio between the pressure drop and the speed of the wire i.e., $X^j = \frac{V^c}{U}$), radii ratio δ, and the Brinkman numbers Br^1 and Br^2 are discussed and drawn in Figures 3-14

Figure 3**Figure 3** shows the effect of slip parameters($\varepsilon D^{2\,(1)}$, $\varepsilon D^{2\,(2)}$) on the velocity profile. It is concluded that the slip parameters enhance the molten polymer inside the pressure die. This observation verifies that the effect of slip parameters increase the velocity profile near the surface of the optical fiber in the region $1 < r < 1.4$

In Figure 4 and Figure **5** illustrate the variation in velocity for various values of Magneto-hydro-dynamics (MHD), porosity, Deborah numbers and velocity ratio respectively. We examine that the velocity field enhances with a raise in these in these parameters. It is noticeable that the fundamental contribution on the velocity field is seen in

Figure 5, when the velocity ratio is higher. Also, for low elasticity ($\boldsymbol{\varepsilon D^{2\,(1)}}$= 0.1 and $\boldsymbol{\varepsilon D^{2\,(2)}}$ = 0.2) the velocity field deviation slightly differs from Newtonian one, but an increasing $\boldsymbol{\varepsilon D^{2\,(1)}}$ and $\boldsymbol{\varepsilon D^{2\,(2)}}$ the velocity profiles become more complemented showing the effects of shear thinning, as shown in Figure 4. It is interesting to notice that a rise in non-Newtonian parameters and slip parameters **results** in increase the velocity in the slightest degree points of the flow domain. Because the velocity of coating fluid is **a** crucial design requirement, slip parameters and non-Newtonian characteristics of fluid could also be used as controlling devices for the desired quality.

The effects of slip parameter and Deborah numbers on the volume flow rate along with increasing the radii ratio is shown in Figure 6 and Figure **7**. From Figure 6, it is noticed that greater the value of radii ratio, the effect of slip parameters on the volume flow rate becomes much more delicate. It is also noticeable that volume flow rate increases on the increment of Deborah numbers in the region $1 < r < 1.4$, and afterwards reverse effect is observed as shown in Figure 7.

Figure 8 depicts the effect of boosting the slip parameters along with increasing radii on the thickness of coated fiber optics. In this scrutiny, the Deborah number is set as $D^{2\,(1)} = 5$, $\varepsilon D^{2\,(2)} = 10$ and the velocity ratio at $X_1 = 1$, and $X_2 = 1.5$ .It shows that for constant values of these parameters, the thickness of the coated fiber optics becomes bold with an increase in slip parameters and radii ratio as well.

Figure 9 reveals the effects on the thickness of coated fiber optics by changing the Deborah numbers and the radii ratio. This also shows that the thickness of the coated fiber optics boosts with increasing in these parameters.
Figure 10 is sketched **to** determine the consequences of radii ratio along with increasing the slip parameters. In both cases, the thickness of the coated fiber optics tends to extend drastically because the level of radii ratio and therefore the slip parameter increase.

In this way ,we can concluded from Figure 8, Figure **9**, Figure **10** that the extended parameters i.e. slip parameters, Deborah numbers and the radii ratio commit to increase the thickness of coated fiber optics, then surely we may use these lengthen parameters to manipulate the thickness of coated fiber optics as a controlling devices for the required quality.

Figure 11, Figure **12**, Figure **13** and Figure **14** expose the temperature distribution revealing the effects of Brinkman numbers, velocity ratio and Deborah numbers.

Figure 11 shows the effects of slip parameters on the temperature distribution. In this analysis, we alter the slip parameters, i.e., $\gamma_1 = 0.5, 1.5, 2.5, 3.5$ and $\gamma_2 = 1, 2, 3, 4$, and fixed the other parameters at the reference values, i.e. $X_1 = 1$, $X_2 = 1.5$, It explain the temperature distribution inversely varies with slip parameters. This variation in temperature distribution is higher in the region $1 < r < 1.4$.

Figure 12 and Figure 13 illustrate the temperature distribution by showing the consequences of Brinkman numbers and Deborah numbers. The effects of Brinkman numbers and Deborah numbers are to enhance the temperature in the region $1 < r < 1.4$ in all circumstances and then the reverse effect is experienced. Thus it is concluded that viscous heating (Br_1 and Br_2) and non-Newtonian property of melt polymer is beneficial in escalating the fluid temperature inside the die near the surface of the optical fiber and it has negative effect near the surface.

Figure 14 illustrates the temperature distribution showing the effects of velocity ratio. The point of thermo-transition occurs in the center of annular zone. Thus it is concluded that the velocity ratio increase the temperature inside the melt polymer used as a coating material near the surface of the optical fiber then it decreases in the region $1.4 < r < 2$.

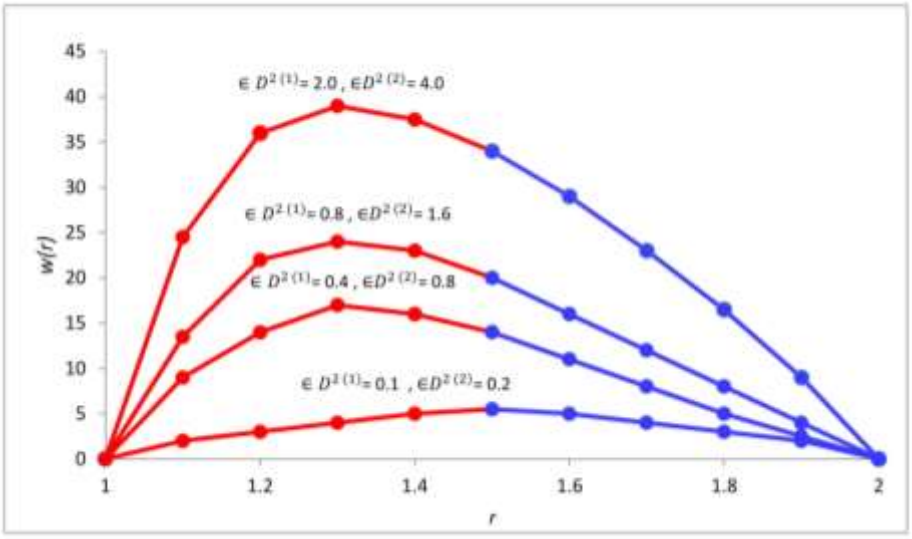

Figure 4

Figure 4: Variation in the velocity field for different inputs of Deborah numbers $\boldsymbol{\varepsilon D^{2\,(1)}}$ ***and*** $\boldsymbol{\varepsilon D^{2\,(2)}}$*, fixing* $\boldsymbol{X_1 = 1, X_2 = 1.5, \gamma_1 = 0.2,\ \gamma_2 = 0.3\ , \gamma = 2,\ \delta = 2,\ M = 0.2,\ \omega = 0.1,\ K_p = 2,\ \Omega = 0.1,\ \mu = 1, 2}$.

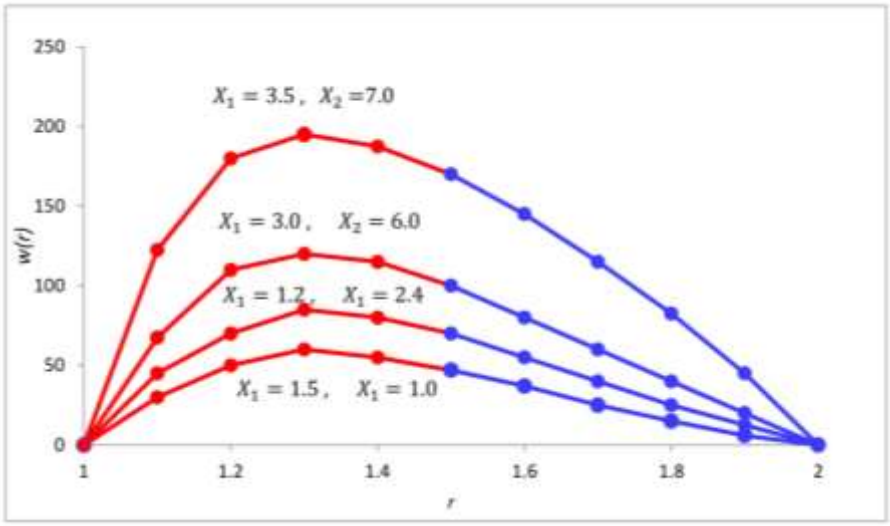

Figure 5

Figure 5: Variation in the velocity field for different inputs of dimensionless parameters $\boldsymbol{X_1}$ ***and*** $\boldsymbol{X_2}$*, fixing* $\boldsymbol{\varepsilon D^{2\,(1)} = 5, X_2 = 10, \gamma_1 = 0.2,\ \gamma_2 = 0.3\ , \delta = 2,\ M = 0.2,\ \omega = 0.1,\ K_p = 2,\ \Omega = 0.1,\ \mu = 1, 2}$.

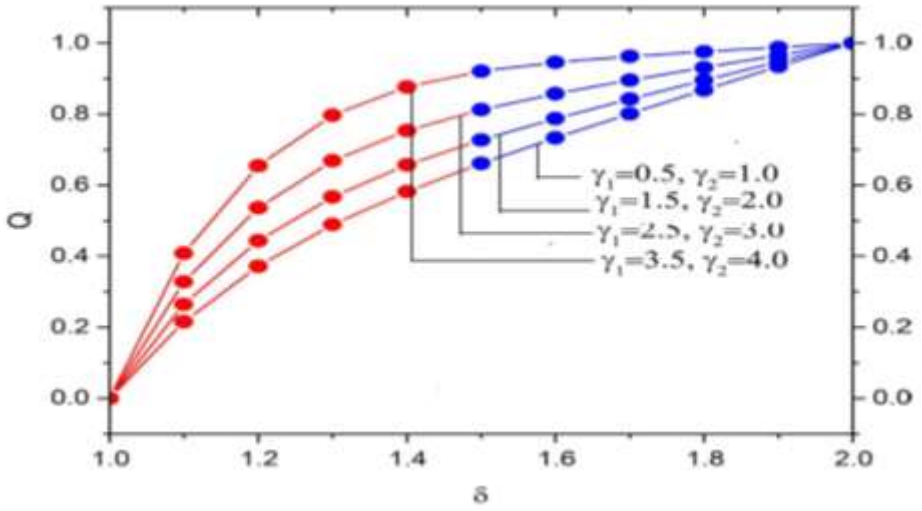

Figure 6

Figure 6: Variation in the volume flow rate for different inputs of Slip parameters $\boldsymbol{\gamma_1}$ *and* $\boldsymbol{\gamma_2}$*, fixing* $\boldsymbol{\varepsilon D^{2\,(1)} = 5}$, $\boldsymbol{\varepsilon D^{2\,(2)} = 10}$, $\boldsymbol{X_1 = 1,\ X_2 = 1.5}$

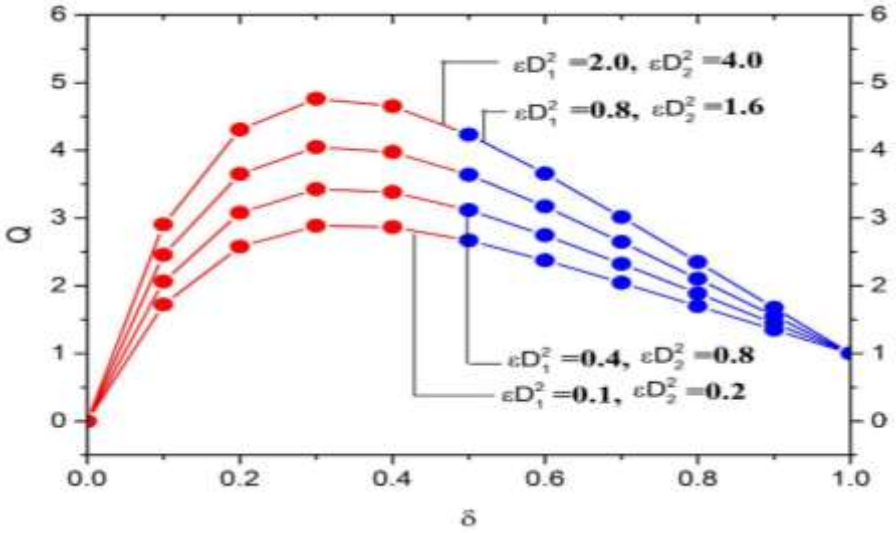

Figure 7

Figure 7: Variation in the Volume flow rate for different inputs of Deborah numbers $\boldsymbol{\varepsilon D^{2\,(1)}}$ *and* $\boldsymbol{\varepsilon D^{2\,(2)}}$ *fixing* $\boldsymbol{X_1 = 1, X_2 = 1.5, \gamma_1 = 0.2,\ \gamma_2 = 0.3}$

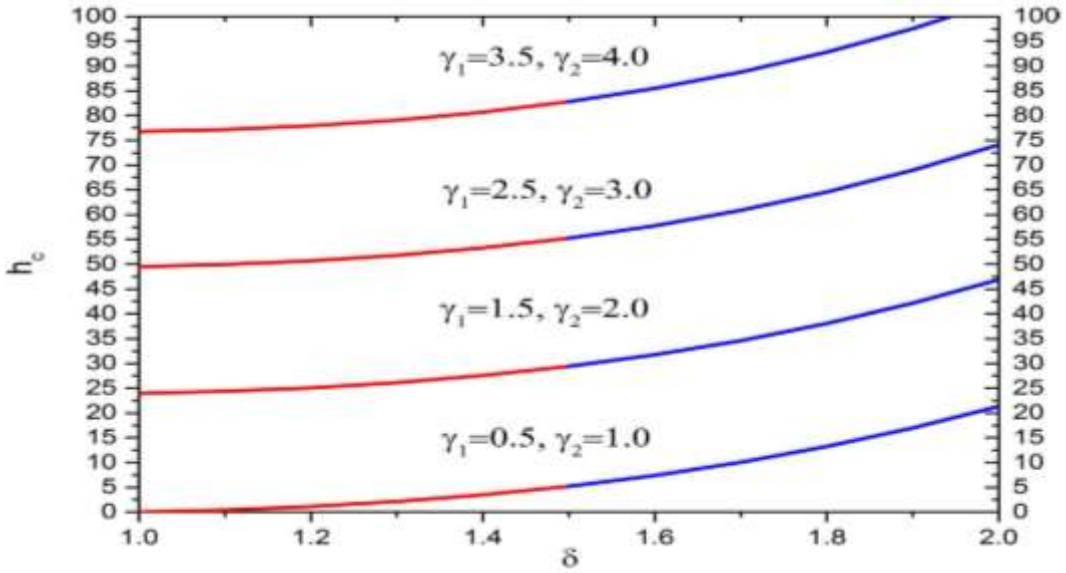

Figure 8

Figure 8: Thickness of coated fiber optics for different inputs of slip parameters $\boldsymbol{\gamma_1}$ ***and*** $\boldsymbol{\gamma_1}$ *fixing* $\boldsymbol{\varepsilon D^{2\,(1)} = 5}$, $\boldsymbol{\varepsilon D^{2\,(2)} = 10}$, $\boldsymbol{X_1 = 1,\ X_2 = 1.5}$

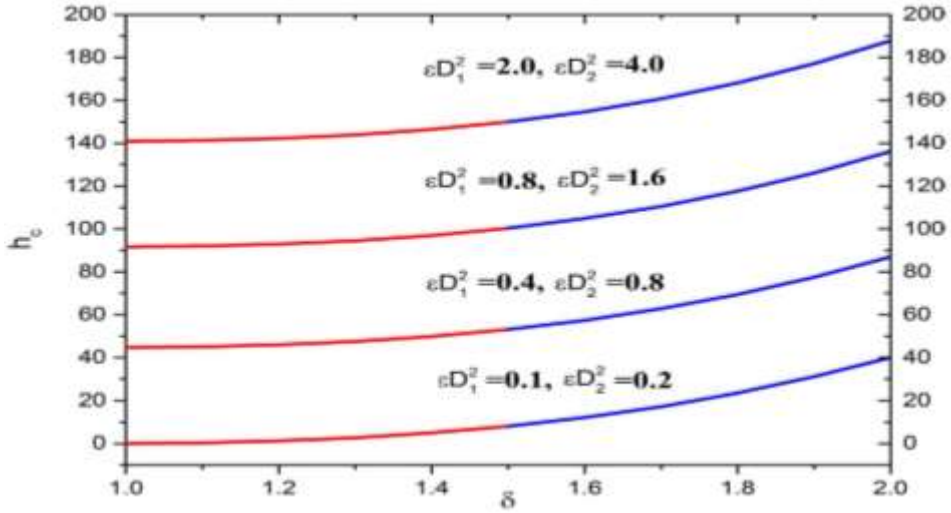

Figure 9

Figure 9: Thickness of coated fiber optics for different inputs of Deborah numbers $\boldsymbol{\varepsilon D^{2\,(1)}}$ ***and*** $\boldsymbol{\varepsilon D^{2\,(2)}}$, *fixing* $\boldsymbol{X_1 = 1, X_2 = 1.5, \gamma_1 = 0.2,\ \gamma_2 = 0.3}$

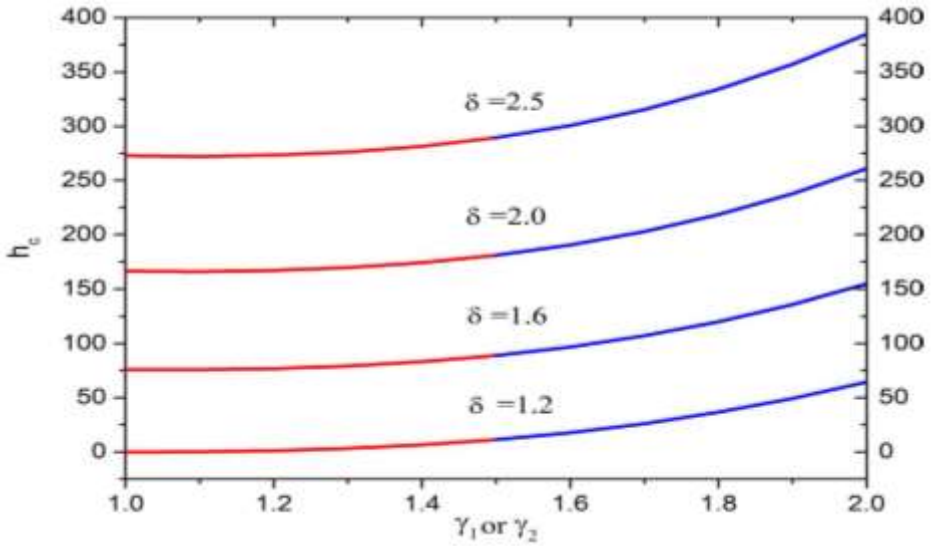

Figure 10

Figure 10 Thickness of coated fiber optics for different inputs of radii ratio $\boldsymbol{\delta}$ *fixing* $\boldsymbol{\varepsilon D^{2\,(1)} = 5}$, $\boldsymbol{\varepsilon D^{2\,(2)} = 10}$, $\boldsymbol{X_1 = 1,\ X_2 = 1.5}$

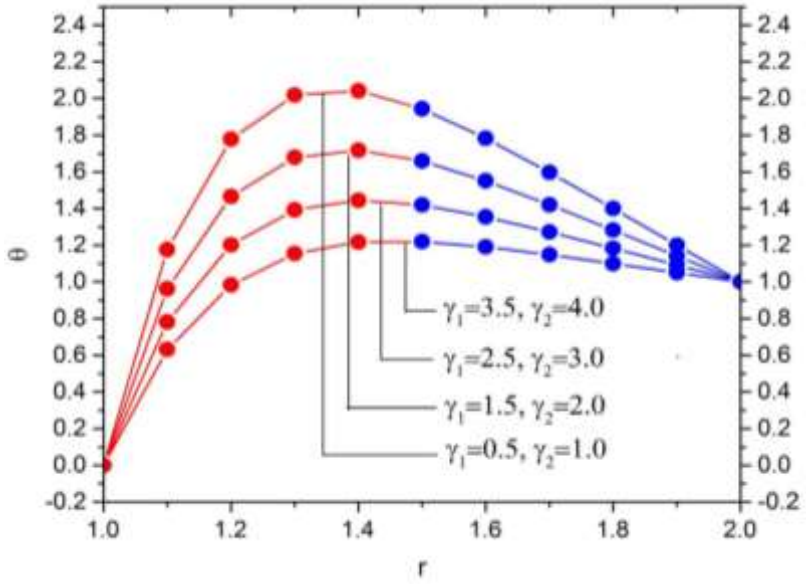

Figure 11

Figure 11: Variation in the Temperature for different inputs of slip parameters $\boldsymbol{\gamma_1}$ *and* $\boldsymbol{\gamma_2}$, *fixing* $\boldsymbol{\varepsilon D^{2\,(1)} = 5}$, $\boldsymbol{\varepsilon D^{2\,(2)} = 10}$, $\boldsymbol{X_1 = 1,\ X_2 = 1.5}$, $\boldsymbol{\delta = 2}$, $\boldsymbol{Br^1 = 5}$, $\boldsymbol{Br^2 = 10}$

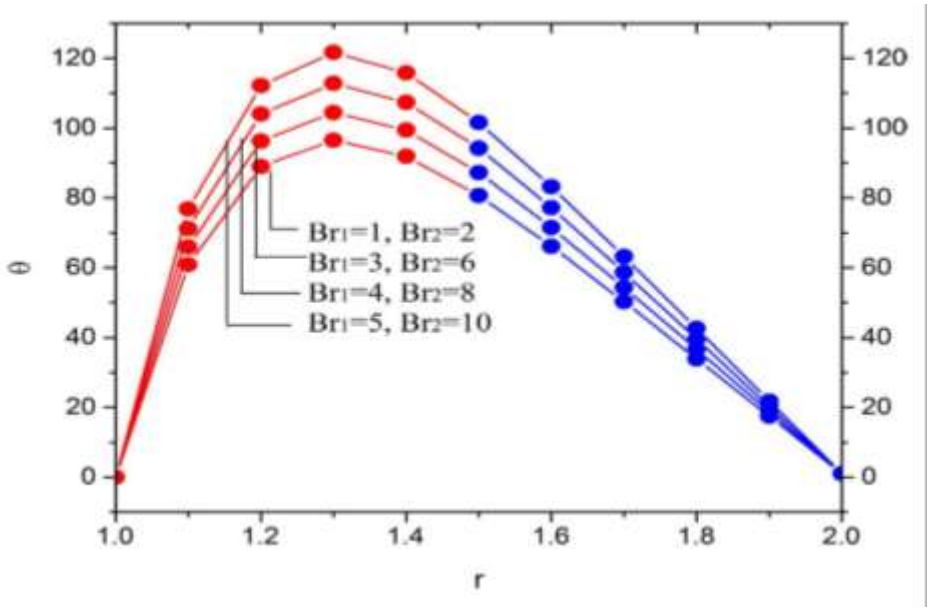

Figure 12

Figure 12: Variation in the Temperature for different inputs of Brinkman numbers $\boldsymbol{Br^1}$ *and* $\boldsymbol{Br^2}$ *, fixing* $\boldsymbol{\varepsilon D^{2\,(1)} = 5}$, $\boldsymbol{\varepsilon D^{2\,(2)} = 10}$, $\boldsymbol{X_1 = 1}$, $\boldsymbol{X_2 = 1.5}$, $\boldsymbol{\delta = 2}$, $\boldsymbol{\gamma_1 = 1}$, $\boldsymbol{\gamma_2 = 5}$

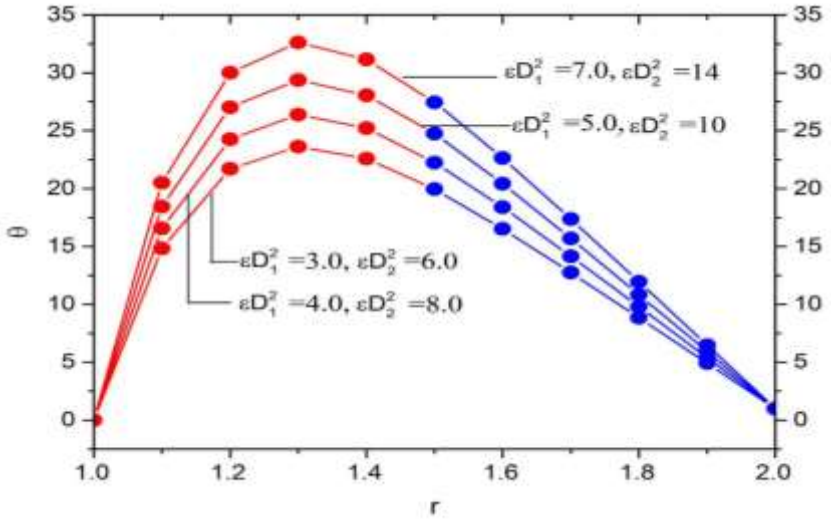

Figure 13

Figure 13: Variation in the Temperature for different inputs of Deborah numbers $\boldsymbol{\varepsilon D^{2\,(1)}}$ *and* $\boldsymbol{\varepsilon D^{2\,(2)}}$, *fixing* $\boldsymbol{X_1 = 1}$, $\boldsymbol{X_2 = 1.5}$, $\boldsymbol{\gamma_1 = 1}$, $\boldsymbol{\gamma_2 = 5}$, $\boldsymbol{\delta = 2}$, $\boldsymbol{Br^1 = 5}$, $\boldsymbol{Br^2 = 4}$

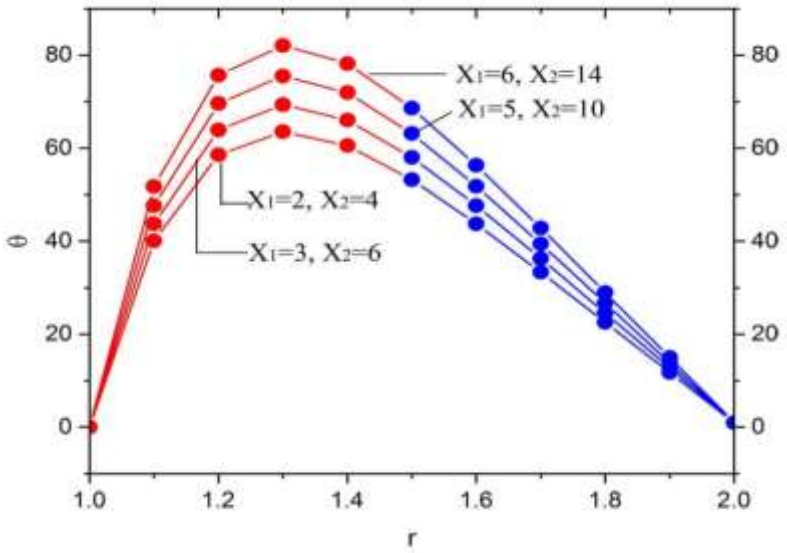

Figure 14

Figure 14: Variation in the Temperature for different inputs of dimensionless parameters $\boldsymbol{X_1 and\ X_2}$ *, fixing* $\boldsymbol{\varepsilon D^{2\,(1)} = 2,\ \ \varepsilon D^{2\,(2)} = 5,\ \ Br^1 = 5,\ \ Br^2 = 4,\ \ \delta = 2,\ \ \gamma_1 = 1,\ \ \gamma_2 = 5}$

CONCLUSION

The solutions are obtained exactly for velocity and temperature distributions, related to double-layer optical fiber coating process using melt polymer satisfying Phan-Thien-Tanner (PTT) fluid model in a pressure type die. The coating of double-layer optical fiber is carried by wet-on-wet process. The results are examined on various pertinent parameters such as Deborah numbers $\varepsilon D^{2\,(1)}$ and $\varepsilon D^{2\,(2)}$, (ratio between the pressure drop and the speed of the wire i.e., $X^j = \frac{V^c}{U}$), radii ratio δ, and the Brinkman numbers Br^1 and Br^2. The slip parameters, Deborah numbers and velocity ratio increase the fluid velocity of the first layer in all circumstances, and then, the reverse effect is experienced. Thus, it is concluded that viscous heating Br^1 and Br^2 and non-Newtonian property of melt polymer is beneficial in escalating the fluid temperature inside the die near the surface of the optical fiber and it has negative effect near the surface. Also, the slip parameters, Deborah numbers and the radii ratio make the increment in the thickness of coated fiber optics, thus we may use these parameters to control the thickness of coated fiber optics as a controlling device for the required quality

Additionally, the effects of Deborah numbers, velocity ratio and the Brinkman numbers enhances the temperature in the region $1 < r < 1.4$ in all circumstances, thereupon a reverse effect is experienced. The effects of slip parameters are much more different to Brinkman numbers i.e. reverse effect is observed. Hence, it is concluded that viscous heating Br^1 and Br^2 and non-Newtonian property of melt polymer is benign in escalating the fluid temperature in the layers near the surface of the optical fiber and having a upheaval in the middle of annular region. Also, it shorten to Maxwell and the linear viscous model be settling ε and λ equal to zero, respectively.

REFERENCES

1. Z.khan, R.A.Shah, S.Islam, Bilal jan, Md.Imran, Farisa. T (2016) Steady flow and heat transfer analysis of Phan-Thein-Tanner fluid in double-layer optical fiber coating analysis with Slip Conditions, *Journal of scientific reports*, Article number. 34593.
2. Sang.H.park, Yeong.S.Lee, Ho Sang.K, (2010) Theoretical prediction on double-layer coating in wet-on-wet optical fiber coating process, *Journal of coatings technology and research (Springer*), Vol.08, pp.35-44

3. A.M.Siddiqui, T.Haroon, H.khan. (2011) wire coating extrusion in a pressure-type die in a flow of a third grade fluid via homotopy perturbation method, *International Journal of nonlinear sciences and numerical simulation*, Vol.10(02), pp.247-258
4. Siddiqui A.M, M.Zeb, T.Haroon and Q.Azim., (2019) Exact solution for the heat transfer of two immiscible PTT fluids flowing in concentric layers through a pipe, *Journal of MDPI (Mathematics*), Vol.7, pp.81-97
5. Kyoung.J.K, Ho sang. K,. , (2012) Analytic Study of Non-Newtonian double-layer coating liquid flows in optical fiber manufacturing. J*ournal of Applied Mechanics and Materials,* Vol.224, pp.260–263.
6. M.Elahi, R.A.shah, A.M.Siddiqui R.A.Shah, T.Haroone (2011) Analytical solutions for heat transfer flows of a third grade fluid in case of post-treatment of wire coating. *International Journal of physical sciences*, Vol.06 (17), pp.4213–4223.
7. S.Asgher, M.Ayub. M.M.Gulzar (2006) Effects of partial slip on flow of a third grade fluid, *Journal of Acta Mehanica Sinica*, Vol.22 (05), pp.393–396.
8. Malashetty, M.S.; Umavathi, J.C., (1997) Two-phase magneto hydro dynamic flow and heat transfer in an inclined channel, *International Journal of Multiphase Flow*, Vol.23, pp.545–560.
9. Siddiqui, A.M.; Azim, Q.A.; Rana, M.A., (2010) On exact solutions of concentric n-layer flows of viscous fluids in a pipe. *Non-linear Science Letters A*, Vol.1, pp.67–76.
10. I.Khan, Zeeshan, T.Gul, S.Islam, R.A.Shah, (2015) Exact solution of PTT fluid in optical fiber coating analysis using Two-layer coating flow. *Journal of applied Environmental and Biological Sciences.* Vol.05 (02), pp.96–105.